Synchronization and control of spatiotemporal chaos using time-series data from local regions

Nita Parekh, V. Ravi Kumar,[a] and B. D. Kulkarni
Chemical Engineering Division, National Chemical Laboratory, Pune - 411 008, India

(Received 23 June 1997; accepted for publication 8 October 1997)

In this paper we show that the analysis of the dynamics in localized regions, i.e., *sub-systems* can be used to characterize the chaotic dynamics and the synchronization ability of the spatiotemporal systems. Using noisy scalar time-series data for driving along with simultaneous self-adaptation of the control parameter representative control goals like suppressing spatiotemporal chaos and synchronization of spatiotemporally chaotic dynamics have been discussed. © *1998 American Institute of Physics.* [S1054-1500(98)01301-9]

Most physical, chemical and biological systems are high-dimensional and exhibit complex spatiotemporal patterns including spatiotemporal chaos.[1] The synchronization and control of the spatiotemporally chaotic dynamics in these systems is currently being investigated and has been reviewed in Refs. 2–11. In this paper we study the synchronization and regulation of the spatiotemporal systems using time-series data from local regions. This approach may help in specifying the requirements of time-series data from the spatial domain for control. Since the phase space is large for spatiotemporal systems it may be worthwhile to first show how the conventional diagnostics for low dimensional systems may be appropriately utilized to study the synchronization behavior of higher-dimensional spatiotemporally chaotic systems. The feasibility of the approach may be seen by studying the behavior of the sub-system invariant properties such as the Lyapunov dimension and Kolmogorov-Sinai (K-S) entropy[12–19] for increasing sub-system size. Important and illustrative control goals, e.g., suppressing spatiotemporal chaos by directing the system to desired stable fixed point or low-period states (servo-control), and dynamical synchronization of the spatiotemporally chaotic systems using localized *sub-system* information have been addressed in this context. The above aims have been carried out for two prototype examples of coupled map lattices (CMLs), *viz.*, the diffusively coupled logistic map (LCML) and the diffusively coupled Henon map (HCML).

I. INTRODUCTION

The first CML studied is obtained by diffusively coupling N logistic maps on a one-dimensional lattice[16] and is defined as

$$x_{n+1}(i)=(1-\epsilon)f(x_n(i))+\frac{\epsilon}{2}[f(x_n(i-1))+f(x_n(i+1))], \tag{1}$$

where, n is the discrete time; i the lattice site, $i=1,2,\ldots,N$; and ϵ the diffusive coupling coefficient. The nonlinear function $f(x)$ is given by the quadratic form

$$f(x_n)\equiv x_{n+1}=1-\alpha x_n^2. \tag{2}$$

Equation (1) exhibits a wide variety of spatiotemporal patterns, viz., periodic, quasiperiodic, chaotic and complex frozen patterns depending on the choice of parameters α and ϵ.[16] In Fig. 1(a) is shown the typical spatiotemporally chaotic dynamics of the LCML (1) for periodic boundary conditions and *random* initial conditions. This complex pattern arises due to interactions between the diffusion and nonlinear mechanisms in the LCML. The bifurcation parameter $\alpha=1.9$ has been chosen such that the local map (2) exhibits temporal chaos (Lyapunov exponent $\lambda\sim 0.55$). The coupling strength chosen was $\epsilon=0.4$.

The second CML considered is the diffusively coupled Henon map lattice in 1-D

$$x_{j,n+1}(i)=(1-\epsilon)f_j(x_{j,n}(i))+\frac{\epsilon}{2}[f_j(x_{j,n}(i-1)+f_j(x_{j,n}(i+1))], \tag{3}$$

where

$$x_{1,n+1}\equiv f_1(x_{1,n},x_{2,n})=1-\alpha x_{1,n}^2+x_{2,n},$$

$$x_{2,n+1}\equiv f_2(x_{1,n},x_{2,n})=\beta x_{1,n}, \tag{4}$$

$j=1,2$; $i=1,2,\ldots N$. Again, the parameter values have been so chosen that the local Henon map exhibits chaotic dynamics ($\alpha=1.4$ and $\beta=0.3$ for which the maximum Lyapunov exponent, $\lambda_{\max}\sim 0.42$).[20] On assuming *identical* initial conditions for $x_{j,0}(i)$, the HCML (3) exhibits spatially homogeneous but temporally chaotic dynamics [as seen in Fig. 1(b) for $n<100$]. On giving random perturbations to the central five lattice sites at $n=100$, a changeover from spatially homogeneous to an inhomogeneous spatiotemporal pattern is observed with the spread of perturbation to the boundaries because of diffusive coupling [Fig. 1(b)]. The following section discusses the analysis of spatiotemporally chaotic dynamics in terms of the sub-system invariant measures. In

[a]Electronic mail: ravi@ncl.ems.res.in

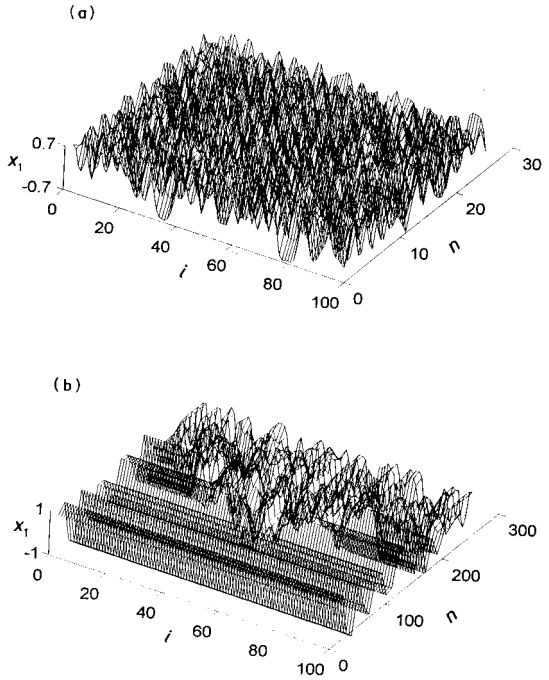

FIG. 1. Spatiotemporal chaos in CMLs for lattice size $N=100$ (every 10th iteration is plotted) : (a) Spatiotemporal dynamics of LCML for $\alpha=1.9$, $\epsilon=0.4$. Random initial conditions were assumed at $n=0$. (b) Spatiotemporal dynamics of HCML for $\alpha=1.4$, $\beta=0.3$, $\epsilon=0.3$. At $n=0$ identical initial conditions were assumed. A finite random perturbation given to the central five lattice sites, at $n=100$ results in the complex spatiotemporal behavior because of coupling.

section III the dynamical synchronization and control of spatiotemporal chaos in these CMLs is discussed for representative goals.

II. ANALYSIS OF SPATIOTEMPORAL DYNAMICS

For a CML of size N, there are mN Lyapunov exponents (m being the number of degrees of freedom in the corresponding single map, i.e., $m=1$ for logistic map and $m=2$ for Henon map) and their computation can be taxing and practically infeasible for large N. However, if attention is restricted to a localized sub-system of size $n_s(<<N)$, the calculation of the Lyapunov exponents is significantly reduced to mn_s. The calculation of these sub-system exponents is similar to those of the full system, that is, by time-averaging the growth rate of linearized orthonormal vectors $\delta\mathbf{x}_n^l$, within the sub-system, and is given by

$$\lambda_l^{(s)}=\limsup_{n\to\infty}\ln\frac{|\delta\mathbf{x}_{n+1}^l|}{|\delta\mathbf{x}_0^l|},\quad l=1\ldots mn_s. \tag{5}$$

While calculating these exponents, the flow of information at the sub-system boundary sites $k=1$ and $k=n_s$, may be treated as (a) noise effects, or, (b) explicitly corrected by evaluating the sub-system Lyapunov exponents only for n_s-2 sites (i.e., excluding the boundary sites). Our calculations of the sub-system Lyapunov exponents, $\lambda_l^{(s)}$ for both treatments (*a*,*b*) were found to be in quantitative agreement with open boundary conditions used for the sub-system dynamics.

Now, from a knowledge of the spectrum of sub-system Lyapunov exponents, $\lambda_i^{(s)}$, the effective sub-system Lyapunov dimension, $d_L^{(s)}$, may be obtained and is defined as

$$d_L^{(s)}=j+\frac{1}{|\lambda_{j+1}^{(s)}|}\sum_{i=1}^{j}\lambda_i^{(s)}, \tag{6}$$

on using the well-known Kaplan and Yorke (KY) conjecture.[21] Here j is the largest integer for which the sum of the exponents, $\lambda_1^{(s)}+\ldots+\lambda_j^{(s)}\geqslant 0$. If $\lambda_1<0$, then $d_L^{(s)}=0$ and if $j=mn_s$, then $d_L^{(s)}=mn_s$.[20] The Lyapunov dimension gives the effective dimensionality of the underlying attractor. The corresponding intensive quantity, the sub-system dimension density, $\rho_d^{(s)}$, may then be defined as

$$\rho_d^{(s)}=\frac{d_L^{(s)}}{n_s}. \tag{7}$$

It gives an estimate of the number of degrees of freedom required to characterize the dynamical behavior of the full spatiotemporal system.

Another important invariant measure is the Kolmogorov-Sinai (KS) entropy and is defined as the sum of positive Lyapunov exponents λ_+.[22] It quantifies the mean information production and growth of uncertainty in a system subjected to small perturbations.[21] For regular predictable behavior, the KS entropy is zero while for chaotic systems it takes a finite positive value, and is infinite for continuous stochastic processes. The sub-system KS-entropy, $h^{(s)}$, is defined as

$$h^{(s)}=\sum\lambda_+^{(s)} \tag{8}$$

and the corresponding density function, the sub-system entropy density, $\rho_h^{(s)}$, is given by

$$\rho_h^{(s)}=\sum\lambda_+^{(s)}/n_s. \tag{9}$$

The dependence of these invariant measures as a function of the sub-system size, n_s is discussed below. In Fig. 2(a) is shown the plot of the sub-system dimension, $d_L^{(s)}$, as a function of its size n_s (solid line corresponds to LCML and the dashed line to HCML). The sub-system dimension $d_L^{(s)}$ is seen to linearly increase with the sub-system size n_s for both the CMLs. This suggests that it may be possible to determine the effective dimensionality of the whole system from sub-system analysis. Further, the saturating behavior of the sub-system dimension density, $\rho^{(s)}$ [Fig. 2(b)] helps in determining the critical sub-system size, n_{sc}, required to predict the dimensionality of the full system. Similar behavior was observed in the sub-system KS entropy, $h^{(s)}$ and the entropy density, $\rho_h^{(s)}$, for increasing sub-system size [Figs. 2(c) and 2(d)]. This implies that though the entropy increases linearly with the sub-system size, the average rate of information loss/gain levels off for $n_s>n_{sc}$. The above relationships were also observed for logistic maps diffusively coupled on a 2-dimensional square lattice of size $N\times N$ (results not shown). These results indicate that it may be possible to analyze the dynamical behavior of reaction-diffusion sys-

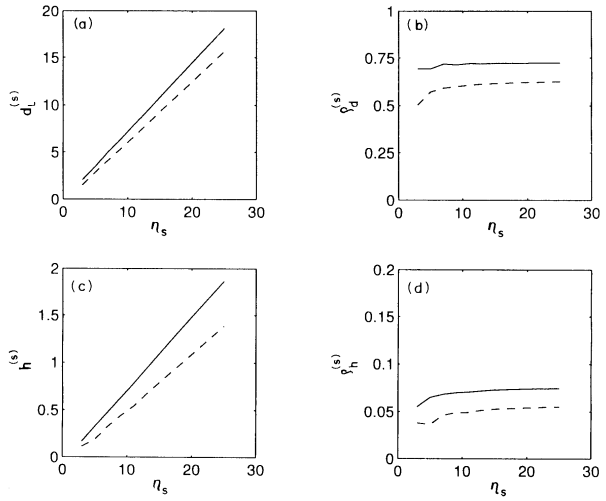

FIG. 2. Behavior of the sub-system invariants as a function of sub-system size n_s for LCML (solid line) and HCML (dashed line) : (a) Lyapunov dimension, $d_L^{(s)}$; (b) dimension density, $\rho_d^{(s)}$; (c) entropy, $h^{(s)}$; (d) normalized entropy, $\rho_h^{(s)}$. Parameters and lattice size identical to Fig. 1.

tems from an analysis of relatively smaller sub-systems. This feature may prove to be computationally very advantageous, especially in higher spatial dimensions.

III. SYNCHRONIZATION AND CONTROL OF SPATIOTEMPORAL CHAOS

In this section, we discuss the synchronization and control of spatiotemporally chaotic dynamics for different goals with the following important factors considered, viz., (1) a mechanism by which a control parameter may be self-adapted so that synchronization in the system and the desirable dynamics becomes possible; (2) allow for restrictions in the availability of scalar time-series signals in the spatial domain; and (3) negate the effects of noise in the time-series data. From recent studies on the dynamical synchronization of low-dimensional chaotic systems it is known that a given system (called the *response*) can be made to follow the dynamics of another system by driving the former with scalar time-series signals from the latter.[23–29] The condition for the synchronization to occur is that the response system should possess negative conditional Lyapunov exponents. Following the results of section II, we would now like to see whether sub-system data may suffice in assessing the synchronization ability of the spatiotemporal system.

Before discussing the results, we present the methodology adopted to synchronize the dynamics of spatiotemporal systems governed by different attractors. For clarity we define the driving system by

$$\mathbf{x}_{n+1}(i)=\mathbf{F}[\mathbf{x}_n(i),\mathbf{x}_n(i\pm1),\alpha,\beta], \tag{10}$$

where $\mathbf{x}_n(i)=x_{j,n}(i)$, $j=1,\ldots,m$ (m denotes the number of degrees of freedom in the local map), and $i=1,\ldots,N$. To incorporate the effects of noise arising due to measurement errors, the sub-system driving signals are assumed to be given by

$$x'_{1,n}(k)=x_{1,n}(k)+\gamma\eta_n(k), \quad k=1,\ldots,n_s, \tag{11}$$

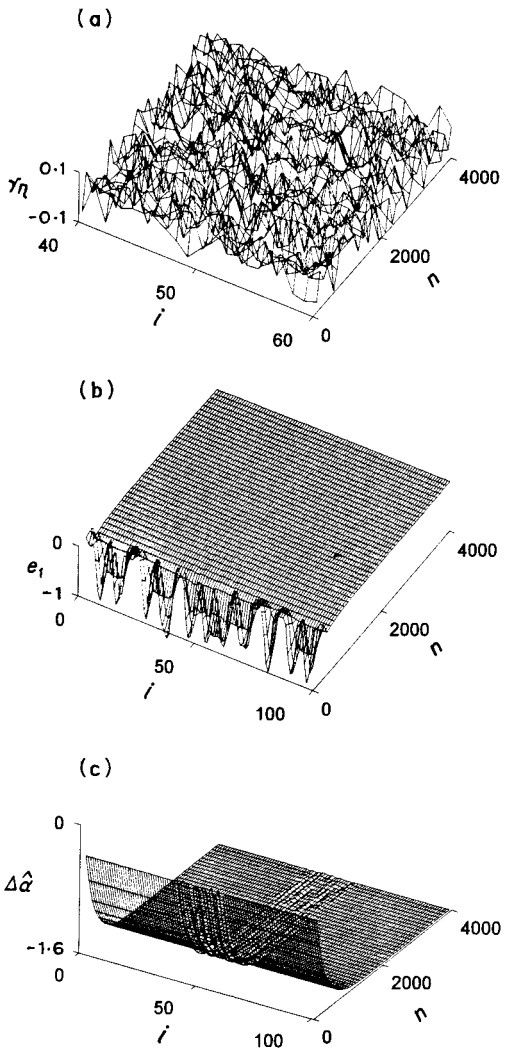

FIG. 3. Stabilization of the spatiotemporally chaotic dynamics with noise reduction for the LCML. The response system ($\hat{\alpha}=1.9$) was assumed to be driven by noisy time-series signals, $x'_{1,n}(k)$, from a sub-system ($n_s=21$) of the process ($\alpha=0.3$). (a) Measurement noise, $\gamma\eta_n(k)=x'_{1,n}(k)-x_{1,n}(k)$, introduced in the monitored sub-system process variables. (b) Space-time behavior of the error signals, $e_1(i)=\hat{x}_{1,n}(i)-x_{1,n}(i)$, $i=1,\ldots,N$. $e_1(i)$ is seen to fall to zero at all the lattice sites indicating complete synchronization of the response dynamics with the process. (c) Space-time plot of the adapter signals, $\Delta\hat{\alpha}$ implemented; stiffness coefficient for adaptation, $\mu=0.01$. Note that at $n=0$, the adapter $\Delta\hat{\alpha}=0.0$ which then eventually assumes an average value of -1.6 (the initial difference between α and $\hat{\alpha}$). The adapter signals continuously filter the noise shown in (a) to achieve the dynamical synchronization seen in (b).

where $\eta_n(k)$ denotes the random noise in the interval (-.5,.5) of strength γ. The response system, written in a different notation from eq. (10), is given by

$$\hat{\mathbf{x}}_{n+1}(i)=\mathbf{F}[\hat{\mathbf{x}}_n(i),\hat{\mathbf{x}}_n(i\pm1),\mathbf{x}'_n(k),\hat{\alpha},\hat{\beta}], \tag{12}$$

where $\hat{\mathbf{x}}_n(i)$ are the corresponding variables, $\hat{\alpha}$ and $\hat{\beta}$ the response parameters, and $\mathbf{x}'_n(k)$, the driving variables. To study the ability of the response system to synchronize its dynamics with that of the driving system (10), we analyzed the conditional Lyapunov exponents for a localized sub-system ($n_s>n_{sc}$). These exponents were calculated by moni-

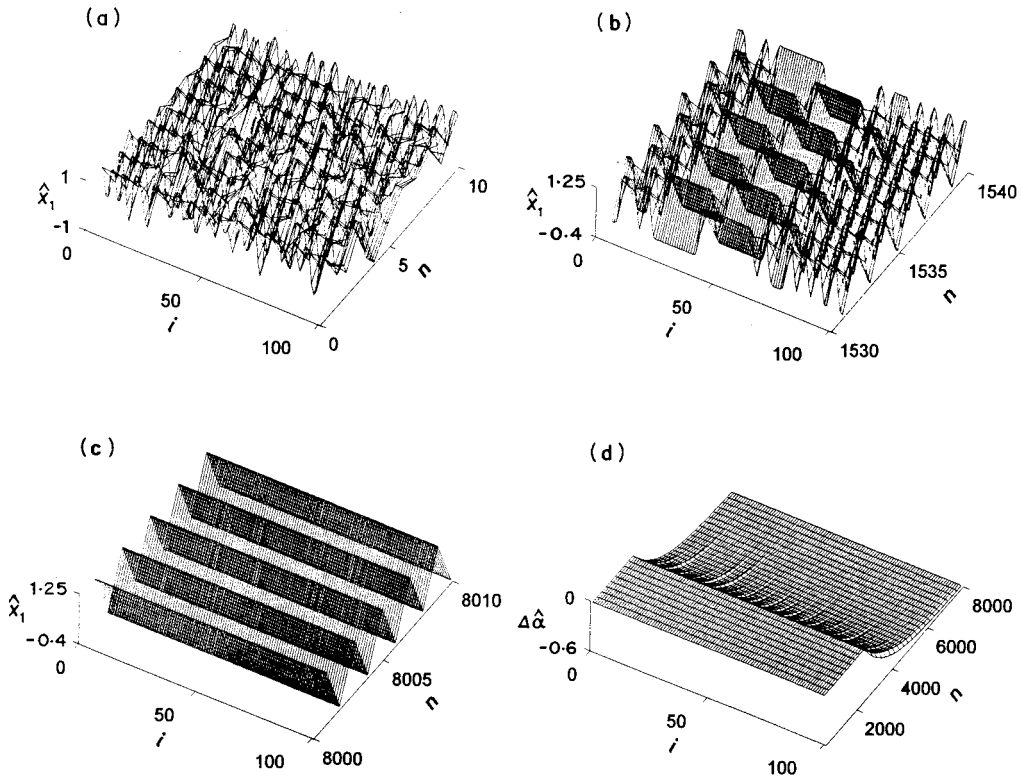

FIG. 4. Controlling the spatiotemporally chaotic dynamics of a response system ($\hat{\alpha}=1.4,\hat{\beta}=0.3$) to temporally 2-period state ($\alpha=0.8,\beta=0.3$). The results are shown for HCML. (a) Spatiotemporally chaotic dynamics of the response system ($\alpha=1.4,\epsilon=0.4$). (b) Spatiotemporal dynamics of the response system on driving it with sub-system time-series signals $x'_{1,n}(k)$, $k=41,\ldots,60$. Self-adaptive mechanism was simultaneously implemented. (c) Oscillatory behavior with phase locking in the spatial domain exhibited by the response system on driving it with time-series signals $x_{1,n}(j)$, $j=5,10,\ldots,100$. (d) Space-time convergence of $\Delta\hat{\alpha}$ to -0.6 for $\mu=0.001$.

toring the growth rate of $(m-1)n_s$ sets of linearized orthonormal vectors obtained on excluding the variables used for driving. For the HCML, the calculations showed that the maximum sub-system conditional exponent is negative on using $x_{1,n}(i)$ as the driving signals indicating possible synchronization. On the other hand, if $x_{2,n}(i)$ were used for driving, the maximum conditional exponent was found to be positive and synchronization is not guaranteed. A synchronization study on HCMLs with different initial conditions but same parameter values (i.e., $\hat{\alpha}=\alpha$, $\hat{\beta}=\beta$) did confirm the above results. It may be also noted that in the case of LCML, the local map being governed by a single variable (i.e., $m=1$) precludes the observance of negative conditional Lyapunov exponents and synchronization in their dynamics is difficult.

However, if driving is carried out on a response system with a different setting of the control parameter, i.e., $\hat{\alpha}\neq\alpha$, then synchronization of the response system dynamics cannot be brought about by driving alone. In this situation, the control parameter $\hat{\alpha}$ needs to be altered appropriately so that synchronization becomes possible. Self-adaptive mechanisms for parametric estimations have been studied in the context of temporal chaotic systems.[30–34] For spatiotemporal systems, the self-adaptation of the control parameter may be carried out as follows. We begin by introducing a space-time dependence in the response control parameter, i.e., $\hat{\alpha}_n(i)$. Initially, the same value of $\hat{\alpha}$ is assumed at all the lattice sites, but different from that of the driving system, i.e., $\hat{\alpha}_0(i)=\hat{\alpha}\neq\alpha$. For the sub-system lattice sites where the signals are available, the parametric corrections, $\Delta\hat{\alpha}_{n+1}(k)$ may be dynamically evaluated as

$$\Delta\hat{\alpha}_{n+1}(k)=\Delta\hat{\alpha}_n(k)+\mu[\hat{x}_{1,n}(k)-x'_{1,n}(k)],\quad k=1,\ldots,n_s, \tag{13}$$

where μ is the stiffness coefficient for adaptation and $\Delta\hat{\alpha}_0(i)=0$. For the lattice sites outside the sub-system an average adaptation, $\Sigma_k\Delta\hat{\alpha}_{n+1}(k)/n_s$, was employed. The response parameter then self-adapts to the desired value α via

$$\hat{\alpha}_{n+1}(i)=\hat{\alpha}_0(i)+\Delta\hat{\alpha}_{n+1}(i),\quad i=1,2,\ldots N. \tag{14}$$

The linear functional form for adaptation considered in eq. (13) is only representative and other functional forms of adaptation, e.g., cubic, history-linear, sign, etc.,[30,33] may be attempted. Further, the choice of μ may be rationalized by studying the stability characteristics of the response and adapter dynamics. As long as the combined system has negative eigenvalues synchronization should be possible. A range of μ values can satisfy this requirement and within this range the specific value of μ will determine the rapidity with which synchronization occurs.

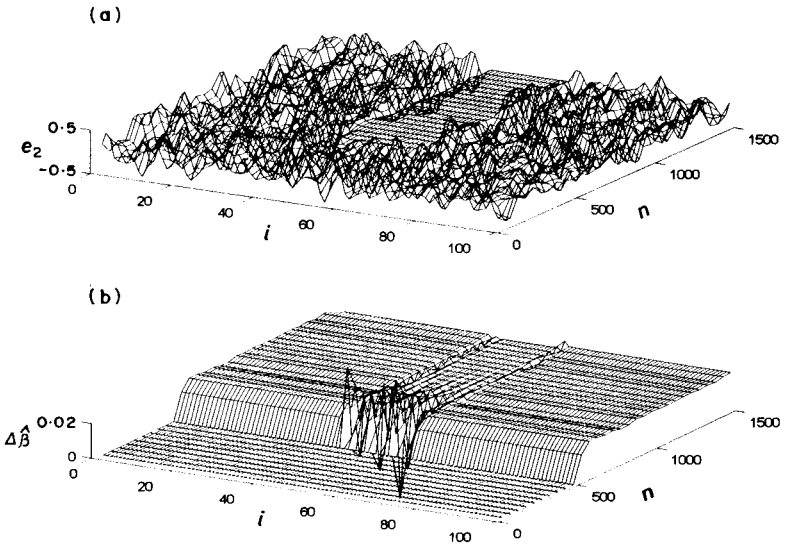

FIG. 5. On using scalar time-series signals, $x_{1,n}(k)$, from a sub-system of HCML exhibiting chaotic dynamics ($\alpha=1.4,\beta=0.3$) to drive the response system ($\hat{\alpha}=1.4$, $\hat{\beta}=0.28$) operating on a different chaotic attractor. (a) Till $n<500$, the error between the non-monitored process and response variables, $e_2=x_{2,n}(i)-\hat{x}_{2,n}(i)$, $i=1,\ldots,N$, is shown without driving or adaptation. Synchronization is obtained only within the sub-system. (b) Space-time behavior of the adapter signals converging to $\Delta\hat{\beta}=0.02$ (the initial difference between β and $\hat{\beta}$).

Using the above methodology, we discuss representative cases pertaining to controlling spatiotemporal chaos. Our first aim was to suppress chaos in a spatiotemporal system and direct it to a desired stable fixed point state via self-adaptation of the control parameter along with simultaneous driving. Noisy time-series signals [shown in Fig. 3(a)] from a sub-system of size $n_s=21$ localized in the central region of the lattice of the driving system ($\alpha=0.3$) were used to drive the spatiotemporally chaotic dynamics of the response system ($\hat{\alpha}_0(i)=1.9$). A rapid space-time synchronization in the dynamics of the response and the driving system is depicted by plotting the error signals $e_n(i)=\hat{x}_n(i)-x'_n(i)$ in Fig. 3(b). The space-time convergent behavior of $\Delta\hat{\alpha}_n(i)$ to a value of -1.6 (the initial difference in the control parameter) by self-adaptation is shown in Fig. 3(c). The fluctuations in $\Delta\hat{\alpha}_n(i)$ is due to the presence of noise in the driving signals which is constantly filtered by the adapter eqs. (13). Thus, the simple form of self-adaptation given in eq. (13) can be effectively used even in the presence of reasonable extents of noise to suppress chaos in the dynamics. The implementation of the driving signals along with the adapter mechanism leads to a faster convergence to the desired stable state. Further, because the final state is a stable one, the system continues to operate in this state even after the driving and self-adaptive mechanism have been switched off. Similar results were also obtained for HCML using scalar sub-system time-series signals (results not shown). These results suggest that it may be possible to suppress chaos in real experimental situations by using scalar time-series signals from a local sub-system with spatial self-adaptation of the control parameter.

Next we considered controlling the spatiotemporally chaotic dynamics to a temporally 2-period state. The sub-system time-series data from an HCML exhibiting spatially homogeneous and temporally periodic oscillations were used to drive the chaotic dynamics of the response [shown in Fig. 4(a)]. On using the self-adaptive mechanism [eq. (13)] along with driving, the desired spatially homogeneous and temporally periodic pattern is observed only within the sub-system [Fig. 4(b)]. Outside the sub-system, the dynamics is not phase synchronized, though oscillating periodically in time. On using driving signals from every 5th lattice site, we were able to obtain complete synchronization with phase locking in the response and the desired system dynamics [Fig. 4(c)]. Thus, though local sub-system data is sufficient to suppress chaos and direct the system to a stable periodic state, for phase synchronization, time-series measurements from the full spatial domain is required (which may be spaced out depending on the complexity of the desired state). The space-time evolution of the parametric correction is shown in Fig. 4(d).

The above studies were focused on directing the system to stable states. Now we discuss the more difficult case of directing a spatiotemporal system from one chaotic state to another. The results in this study are presented for the HCML [eqs. (3),(4)] with sub-system driving signals used to evaluate parametric corrections $\Delta\hat{\beta}$ in the alternate control parameter $\hat{\beta}$. This was carried out in a procedure identical to evaluating $\Delta\hat{\alpha}$ and $\hat{\alpha}$ [eqs. (13),(14)] in Figs. 3, and 4. In this case, synchronization was possible only within the sub-system [Fig. 5(a)], even though the response system control parameter had been appropriately self-adapted [Fig. 5(b)]. The asynchronous behavior outside the sub-system is because of the sensitive dependence of the chaotic dynamics to initial conditions and suggests that driving signals from the entire spatial domain will be required for complete synchronization in this case and was confirmed (results not shown).

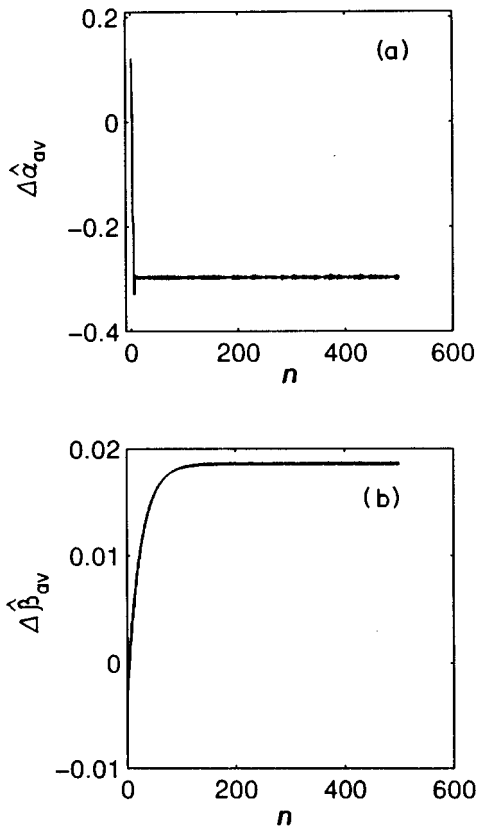

FIG. 6. Simultaneous estimation of both the parameters in HCML using only sub-system time-series signals. The average parametric corrections, $\Delta\hat{\alpha}_{av}$ and $\Delta\hat{\beta}_{av}$ implemented over the entire spatial domain are shown. These values, respectively, converge to -0.3 ± 0.01 and 0.02 ± 0.001 for $\mu_1=1.0$ and $\mu_2=-0.1$.

Apart from estimating a control parameter, in many situations, it would be desirable to accurately estimate other intrinsic system parameters. Such a situation can arise when the other parameters of the response system are not known *a priori*.[33–35] Here we show that self-adaptation of two parameters is simultaneously possible on using time-series signals only from a sub-system. In this study both the response system parameters $\hat{\alpha}_0$ and $\hat{\beta}_0$ were set differently from the driving system ($\alpha=1.1,\beta=0.3$, $\hat{\alpha}_0=1.4,\hat{\beta}_0=0.28$). The parametric corrections $\Delta\hat{\alpha}$ and $\Delta\hat{\beta}$ were then simultaneously estimated by using the following two sets of adapter equations within the sub-system

$$\Delta\hat{\alpha}_{n+1}(k)=\Delta\hat{\alpha}_n(k)+\mu_1[\hat{x}_{1,n}(k)-x_{1,n}(k)],$$
$$\Delta\hat{\beta}_{n+1}(k)=\Delta\hat{\beta}_n(k)+\mu_2[\hat{x}_{2,n}(k)-x_{2,n}(k)], \qquad (15)$$

with μ_1 and μ_2 the stiffness coefficients for adaptation, and $k=1,\ldots,n_s$. As before, average corrections, $\Sigma_k\Delta\hat{\alpha}_{n+1}(k)/n_s$ and $\Sigma_k\Delta\hat{\beta}_{n+1}(k)/n_s$ were implemented outside the sub-system. The simultaneous convergence of $\Delta\hat{\alpha}_n\rightarrow-0.3$ and $\Delta\hat{\beta}_n\rightarrow0.02$ in Figs. 6(a), 6(b) suggest that multiparameter estimation may be possible in high-dimensional chaotic systems. Although driving signals in both the variables in the sub-system were necessary for accuracy, there exists a range of μ_1 and μ_2 values wherein multiparameter self-adaptation was successful. Considerable potential exists in applying this technique in accurately characterizing available mathematical models of an experimental system. Using experimental time-series data from a sub-system, the parameter values in the mathematical model (now the response system) can thus be ascertained.

IV. CONCLUSION

To summarize, the interesting scaling relationships that exist in the sub-system invariant properties as a function of increasing sub-system size have been used to study the synchronization properties of high-dimensional spatiotemporal chaotic systems in a simpler fashion. Our results show that suppressing spatiotemporal chaos and controlling the system in desired stable fixed or low-period states is possible using only sub-system data via self-tuning of a control parameter. Simultaneous adaptation of more than one parameters using only sub-system information is also possible. These results allow for relaxation in the monitoring of time-series data from the spatial domain for control purposes. On the other hand, the synchronization studies with chaotic spatiotemporal dynamics suggest that synchronization may be possible only in regions from which time-series data is available.

ACKNOWLEDGMENTS

We gratefully acknowledge the financial support of the Department of Science and Technology, New Delhi, India, in carrying out this work. One of the authors, N.P., would like to acknowledge CSIR, India for financial support.

[1] M. C. Cross and P. C. Hohenberg, Rev. Mod. Phys. **65**, 851 (1993).
[2] T. Shinbrot, Adv. Phys. **44**, 73 (1995).
[3] T. Shinbrot, C. Grebogi, E. Ott, and J. A. Yorke, Nature (London) **363**, 411 (1993).
[4] G. Chen and X. Dong, Int. J. Bifurc. Chaos **3**, 1363 (1993).
[5] J. F. Lindner, B. K. Meadows, W. L. Ditto, M. E. Inchiosa, and A. R. Bulsara, Phys. Rev. Lett. **75**, 3 (1995).
[6] Y. C. Lai and C. Grebogi, Phys. Rev. E **52**, 1894 (1994).
[7] C. B. Muratov, Phys. Rev. E **55**, 1463 (1997).
[8] M. N. Lorenzo, I. P. Marino, V. Perez-Munuzuri, M. A. Matias, and V. Perez-Villar, Phys. Rev. E **54**, R3094 (1997).
[9] I. Aranson, H. Levine, and L. Tsimring, Phys. Rev. Lett. **72**, 2561 (1994).
[10] J. H. Peng, E. J. Ding, M. Ding, and W. Yang, Phys. Rev. Lett. **76**, 904 (1996).
[11] D. Auerbach, Phys. Rev. Lett. **72**, 1184 (1994).
[12] M. C. Cross and P. C. Hohenberg, Science **263**, 1569 (1994).
[13] M. Bauer, H. Heng, and W. Martienssen, Phys. Rev. Lett. **71**, 521 (1993).
[14] J. Argyris, G. Faust, and M. Haase, *An Exploration of Chaos* (Elsevier Science, Amsterdam, 1994).
[15] H. D. I. Abarbanel, R. Brown, J. J. Sidorowich, and L. Tsimring, Rev. Mod. Phys. **65**, 1331 (1993).
[16] K. Kaneko, Prog. Theor. Phys. **72**, 480 (1984); Physica D **23**, 436 (1986); **34**, 1 (1989); Chaos **2** No. 3 (1992) (special issue on coupled map lattices) and references therein.
[17] P. Grassberger, Phys. Scr. **40**, 346 (1989).
[18] G. Mayer-Kress and K. Kaneko, J. Stat. Phys. **54**, 1489 (1989).
[19] J. Warncke, M. Bauer, and W. Martienssen, Europhys. Lett. **25**, 323 (1994).
[20] S. N. Rasband, *Chaotic Dynamics of Nonlinear Systems* (Wiley-Interscience, New York, 1989).
[21] J. L. Kaplan and J. A. Yorke, Lect. Notes Math. **730**, 204 (1979).
[22] Y. B. Pesin, Russ. Math. Surveys **32**, 55 (1977).
[23] H. Fujisaka and T. Yamada, Prog. Theor. Phys. **69**, 32 (1983).

[24] L. M. Pecora and T. L. Carroll, Phys. Rev. Lett. **64**, 821 (1990); Phys. Rev. A **44**, 2374 (1991).
[25] R. He and P. G. Vaidya, Phys. Rev. A **46**, 7387 (1992).
[26] M. Ding and E. Ott, Phys. Rev. E **49**, R945 (1994).
[27] K. M. Cuomo and A. V. Oppenheim, Phys. Rev. Lett. **71**, 65 (1993).
[28] C. W. Wu and L. O. Chua, Int. J. Bifurc. Chaos **4**, 979 (1994).
[29] J. F. Heagy, T. L. Carroll, and L. M. Pecora, Phys. Rev. E **50**, 1874 (1994).
[30] B. A. Huberman and E. Lumer, IEEE Trans. Circ. Syst. **37**, 547 (1990); S. Sinha and R. Ramaswamy, Physica D **43**, 118 (1990).
[31] V. Ravi Kumar, B. D. Kulkarni, and P. B. Deshpande, Proc. R. Soc. London, Ser. A **433**, 711 (1991); J. K. Bandyopadhyay, V. Ravi Kumar, B. D. Kulkarni, and P. Bhattacharya, Chem. Eng. Sci. **48**, 3545 (1993).
[32] H. K. Qammer, F. Mossayebi, and L. Murphy, Phys. Lett. A **178**, 279 (1993).
[33] D. Vassiliadis, Physica D **71**, 319 (1994).
[34] U. Parlitz, Phys. Rev. Lett. **76**, 1232 (1996); Int. J. Bifurc. Chaos **6**, 581 (1996).
[35] E. Baake, M. Baake, H. G. Bock, and K. M. Briggs, Phys. Rev. A **45**, 5524 (1992).